

Zeitschrift: IABSE proceedings = Mémoires AIPC = IVBH Abhandlungen
Band: 2 (1978)
Heft: P-12: Time-dependent behaviour of reinforced concrete slabs

Artikel: Time-dependent behaviour of reinforced concrete slabs
Autor: Gilbert, R.I. / Warner, R.F.
DOI: <https://doi.org/10.5169/seals-33216>

Nutzungsbedingungen

Die ETH-Bibliothek ist die Anbieterin der digitalisierten Zeitschriften auf E-Periodica. Sie besitzt keine Urheberrechte an den Zeitschriften und ist nicht verantwortlich für deren Inhalte. Die Rechte liegen in der Regel bei den Herausgebern beziehungsweise den externen Rechteinhabern. Das Veröffentlichen von Bildern in Print- und Online-Publikationen sowie auf Social Media-Kanälen oder Webseiten ist nur mit vorheriger Genehmigung der Rechteinhaber erlaubt. [Mehr erfahren](#)

Conditions d'utilisation

L'ETH Library est le fournisseur des revues numérisées. Elle ne détient aucun droit d'auteur sur les revues et n'est pas responsable de leur contenu. En règle générale, les droits sont détenus par les éditeurs ou les détenteurs de droits externes. La reproduction d'images dans des publications imprimées ou en ligne ainsi que sur des canaux de médias sociaux ou des sites web n'est autorisée qu'avec l'accord préalable des détenteurs des droits. [En savoir plus](#)

Terms of use

The ETH Library is the provider of the digitised journals. It does not own any copyrights to the journals and is not responsible for their content. The rights usually lie with the publishers or the external rights holders. Publishing images in print and online publications, as well as on social media channels or websites, is only permitted with the prior consent of the rights holders. [Find out more](#)

Download PDF: 12.03.2026

ETH-Bibliothek Zürich, E-Periodica, <https://www.e-periodica.ch>

Time-Dependent Behaviour of Reinforced Concrete Slabs

Comportement dans le temps de dalles en béton armé

Langzeitverhalten von Stahlbetonplatten

R. I. Gilbert

R. F. Warner

Teaching Fellow

Professor

University of New South Wales

Sydney, Australia

SUMMARY

A non-linear, layered finite element model for predicting the time dependent behaviour of reinforced concrete slabs under sustained transverse loading, is presented. The effects of biaxial creep and shrinkage are accounted for using a difference formulation of a non-linear creep model and an incremental relaxation type solution procedure. Agreement between theoretical calculations and deflection measurements from an in-service reinforced concrete floor slab and laboratory controlled beam tests is shown to be good.

RÉSUMÉ

L'étude présente un modèle non linéaire d'éléments finis en différentes couches pour l'évaluation du comportement dans le temps de dalles en béton armé sous l'effet de charges permanentes transversales. Un modèle différentiel non linéaire de fluage et une formulation du problème en termes de relaxation permettent de tenir compte des effets biaxiaux du fluage et du retrait. Des mesures de déformations effectuées sur une dalle en service en béton armé et des essais en laboratoire, montrent une bonne concordance avec les calculs.

ZUSAMMENFASSUNG

Es wird gezeigt, wie das Langzeitverhalten von Stahlbetonplatten unter ständigen Lasten mit Hilfe von nichtlinearen, geschichteten finiten Elementen vorhergesagt werden kann. Das zweiachsiges Kriechen und Schwinden des Betons wird dabei mittels eines Differenzen-Verfahrens für nichtlineares Kriechen sowie mit Hilfe eines auf schrittweiser Näherung beruhenden Rechenverfahrens eingeführt. Die Übereinstimmung zwischen theoretischen Werten und Messungen an einer im Betrieb stehenden Platte und an Versuchsbalken ist gut.



1. INTRODUCTION

The finite element method has been widely used to study the short-term behaviour of reinforced concrete slabs. However, the time-dependent behaviour of slabs under sustained load and the effects of biaxial creep and shrinkage have received little research attention, either theoretically or experimentally [6].

In an earlier report, the authors reviewed previous finite element studies of slabs. A layered finite element model was also used to predict the instantaneous, non-linear response of reinforced concrete slabs under transverse loading [3]. The present paper describes an extension of that work to treat time-dependent effects in reinforced concrete slabs. Although directed primarily towards long-term service-load behaviour, the extended model can be used to predict the time-varying behaviour of slabs subjected to any variable history of loading including both service loads and overloads.

A non-linear discrete element analysis is used in which the finite elements are subdivided into layers, each of which may or may not contain steel reinforcement. The different stages of instantaneous material behaviour, including elastic strain, tensile cracking of the concrete, tension stiffening of the intact concrete between the cracks in the tension zone, compressive yielding of the concrete and yielding of the steel reinforcement, are represented by suitable biaxial stress-strain relations for each layer of each element. Compatibility of deformations between the concrete and steel and perfect shear bond between the layers is assumed.

A method of temporal discretisation is employed, whereby creep and shrinkage strains in any chosen time increment are calculated from a non-linear constitutive relation and then introduced into the slab analysis by a direct 'relaxation' type procedure [1].

Theoretical calculations are found to agree well with test results previously obtained from an existing reinforced concrete flat slab building and from laboratory controlled beam tests.

2. BIAXIAL CONSTITUTIVE RELATIONS

A non-linear creep model for concrete under time-varying axial stress has been generalised to treat the case of biaxial stress which occurs in slabs. The basic difference formulation was originally used in studies of time-varying behaviour of beams and columns [9, 10], and has more recently been used in the analysis of long-term behaviour of indeterminate concrete beams and frames [5]. As the uniaxial creep model has already been described [10], only details of the extension to two dimensional stress states will be mentioned here.

A typical, thin concrete slice of a rectangular finite element is considered. At any time t after first loading, the vector of total concrete strain is assumed to consist of component vectors of instantaneous, creep and shrinkage strains:

$$\{\epsilon(t)\} = \{\epsilon^i(t)\} + \{\epsilon^c(t)\} + \{\epsilon^{sh}(t)\} \quad (1)$$

or

$$\begin{bmatrix} \epsilon_x(t) \\ \epsilon_y(t) \\ \epsilon_{xy}(t) \end{bmatrix} = \begin{bmatrix} \epsilon_x^i(t) \\ \epsilon_y^i(t) \\ \epsilon_{xy}^i(t) \end{bmatrix} + \begin{bmatrix} \epsilon_x^c(t) \\ \epsilon_y^c(t) \\ \epsilon_{xy}^c(t) \end{bmatrix} + \begin{bmatrix} \epsilon_x^{sh}(t) \\ \epsilon_y^{sh}(t) \\ \epsilon_{xy}^{sh}(t) \end{bmatrix}$$

In order to model the short-term material non-linearities, the instantaneous strains are taken to consist of a linear-elastic, fully recoverable component, $\{\epsilon^{e\lambda}(t)\}$, and a non-recoverable plastic component, $\{\epsilon^{p\lambda}(t)\}$:

$$\{\epsilon^i(t)\} = \{\epsilon^{e\lambda}(t)\} + \{\epsilon^{p\lambda}(t)\} \quad (2)$$

Although these instantaneous strain components are not directly dependent on time, additional increments of 'instantaneous' strain may occur after loading, due to time dependent cracking caused by shrinkage. Full details of the instantaneous stress-strain relations for the various non-linear material states have been discussed elsewhere [3], and only a brief description will be included here.

Experimental investigations [4] have shown that the strength of concrete under biaxial compression is greater than the uniaxial compressive strength, while the strength of concrete under biaxial tension is independent of the principal stress ratio and equals the uniaxial tensile strength. Concrete is here assumed to be elastic-plastic in compression with compressive yielding governed by the von Mises criterion and associated flow rule. This is slightly more conservative than the experimental yield surface for concrete in the biaxial stress state [4], but is an acceptable approximation in under-reinforced slabs under service conditions.

A maximum normal stress criterion is assumed to govern tensile cracking of the concrete. Cracking occurs in a direction perpendicular to the major principal stress, σ_1 , when σ_1 reaches the uniaxial tensile strength. After cracking, the total tensile force is transferred across each crack by the tensile steel but between the cracks the tensile concrete carries stress locally, mainly in the direction of the steel bars, due to the bond between the concrete and the reinforcement. This 'tension stiffening' effect contributes significantly to the bending stiffness of slabs in the post-cracking range.

Various methods for treating the tension stiffening effect in slabs have been examined elsewhere [3], including the use of average unloading stress-strain relations for concrete after cracking. A simple, alternative procedure was developed, which relies on an adjustment of the stiffness of the tensile steel in regions of cracked concrete. This method has been found to give accurate results in economic solution times, and has been adopted here. After cracking, the concrete is thus assumed not to carry stress perpendicular to the crack direction, but an additional stress in the steel accounts for the total internal tensile force carried by the concrete between the cracks, conveniently lumped at the level of the steel and oriented in the direction of the bars.

The reinforcing steel is assumed to be elastic-plastic in both tension and compression, with stiffness only in the bar directions. When the total strain in the direction of the reinforcement exceeds the yield strain, the steel in this direction is assumed to have yielded. If unloading of the steel occurs after yielding, the unloading branch of the stress-strain curve has a slope equal to the elastic modulus of steel.

The concrete creep strains are assumed to consist of three components: a fully hardening and non-recoverable 'Dischinger' component, $\{\epsilon^d(t)\}$; a non-hardening but fully recoverable viscoelastic component, $\{\epsilon^v(t)\}$; and a component which takes into account non-linear effects at high stress levels, $\{\epsilon^n(t)\}$:

$$\{\epsilon^c(t)\} = \{\epsilon^d(t)\} + \{\epsilon^v(t)\} + \{\epsilon^n(t)\} \quad (3)$$

An increment $\{\Delta\epsilon^c(t_n)\}$ in the creep strain vector, which occurs during the small



time increment Δt between the times t_n and t_{n+1} , depends on the principal stresses, $\{\sigma_p(t_n)\}$, existing at the beginning of the time increment. The vector of elastic, instantaneous, stress-related strains in the principal stress directions at t_n is:

$$\{\epsilon_p^{el}(t_n)\} = \begin{bmatrix} \frac{1}{E_c(t_n)} & -\frac{\nu_c(t_n)}{E_c(t_n)} & \cdot \\ -\frac{\nu_c(t_n)}{E_c(t_n)} & \frac{1}{E_c(t_n)} & \cdot \\ \cdot & \cdot & \cdot \end{bmatrix} \cdot \{\sigma_p(t_n)\} \quad (4)$$

The elastic modulus and the creep Poisson's ratio of concrete at t_n , ie $E_c(t_n)$ and $\nu_c(t_n)$, are considered constant throughout the analysis.

The increments in the two linear components of creep are calculated from the elastic instantaneous strains in the principal stress directions and from the creep properties of the concrete as follows:

$$\{\Delta\epsilon_p^v(t_n)\} = [\{\epsilon_p^{el}(t_n)\} \cdot \phi_*^v - \{\epsilon_p^v(t_n)\}] \frac{\Delta t}{T_v} \quad (5)$$

$$\{\Delta\epsilon_p^d(t_n)\} = \{\epsilon_p^{el}(t_n)\} \cdot \Delta\phi^d(t_n) \quad (6)$$

The terms T_v and ϕ_*^v are constant creep parameters associated with the visco-elastic component, and $\Delta\phi^d(t_n)$ is an increment in a Dischinger-type creep function $\phi^d(t_n)$. Numerical values for all these quantities are obtained from constant stress creep tests carried out in the low-stress linear range where the total creep consists of only two components:

$$\epsilon^c(t) = \epsilon^v(t) + \epsilon^d(t) \quad (7)$$

Upon completion of all creep, ie at time infinity, we have:

$$\epsilon^c(\infty) = \epsilon_*^c = \epsilon_*^v + \epsilon_*^d \quad (8)$$

Two creep functions $\phi(t)$ and $\phi^d(t)$ are derived from the creep terms $\epsilon^c(t)$ and $\epsilon^d(t)$ by dividing by the linear elastic component of instantaneous strain, ϵ^{el} :

$$\phi(t) = \frac{\epsilon^c(t)}{\epsilon^{el}} \quad (9)$$

$$\phi^d(t) = \frac{\epsilon^d(t)}{\epsilon^{el}} = \frac{\epsilon^c(t) - \epsilon^v(t)}{\epsilon^{el}} \quad (10)$$

At time infinity, the final values are

$$\phi_* = \frac{\epsilon_*^c}{\epsilon^{el}} \quad (11)$$

$$\phi_*^d = \frac{\epsilon_*^d}{\epsilon^{el}} \quad (12)$$



The constant parameter ϕ_*^V is likewise defined:

$$\phi_*^V = \frac{\epsilon_*^V}{\epsilon e^{\ell}} \quad (13)$$

So that the following relations apply:

$$\phi_*^d = \alpha_d \cdot \phi_* \quad (14)$$

$$\phi_*^V = (1 - \alpha_d) \cdot \phi_* \quad (15)$$

An exponential relation is used as an approximate representation of viscoelastic creep under constant stress:

$$\epsilon^V(t) = \epsilon e^{\ell} \cdot \phi_*^V (1 - e^{-t/T_V}) \quad (16)$$

The creep function $\phi^d(t)$ can now be evaluated from experimental data:

$$\phi^d(t) = \phi(t) - \phi_*^V (1 - e^{-t/T_V}) \quad (17)$$

The non-linear component of creep strain is assumed to be zero whenever a principal stress is less than a prescribed critical value, σ_c . When a principal stress exceeds σ_c , a power function of stress is used to evaluate the non-linear creep in the principal stress directions:

$$\{\Delta\epsilon_p^n(t_n)\} = [\{\Delta\epsilon_p^d(t_n)\} + \{\Delta\epsilon_p^V(t_n)\}] \cdot f(\sigma) \quad (18)$$

$$\text{and for } \sigma_1 \leq \sigma_c \quad f(\sigma) = 0 \quad (19)$$

$$\sigma_c < \sigma_1 \quad f(\sigma) = \alpha_n \left[\frac{\sigma_1 - \sigma_c}{\sigma_0 - \sigma_c} \right]^n \quad (20)$$

σ_1 is any principal stress greater than σ_c ; σ_0 is the uniaxial compressive strength of concrete; α_n and n are open parameters to be determined from available test data.

With the material parameters α_d , α_n , n and T_V , together with the creep function $\phi(t)$, evaluated from test data, the increment in the vector of creep strains developed in a typical concrete layer during a small time increment in the principal stress directions can be calculated:

$$\{\Delta\epsilon_p^C(t_n)\} = \{\Delta\epsilon_p^d(t_n)\} + \{\Delta\epsilon_p^V(t_n)\} + \{\Delta\epsilon_p^n(t_n)\} \quad (21)$$

The increment in the creep strains in the global coordinate directions is obtained from the following strain transformation:

$$\{\Delta\epsilon^C(t_n)\} = [T_\epsilon] \cdot \{\Delta\epsilon_p^C(t_n)\} \quad (22)$$

$$[T_\epsilon] = \begin{bmatrix} c^2 & s^2 & cs \\ s^2 & c^2 & -cs \\ -2cs & 2cs & c^2 - s^2 \end{bmatrix} \quad (23)$$

In Eq. 23 $c = \cos \theta$; $s = \sin \theta$; and θ is the angle between the maximum principal stress direction and the global coordinate axis.



It is here assumed that the curve of shrinkage strain versus time is affine with the total creep-time curve for constant stress. The shrinkage strain developed during the small time increment Δt in each global coordinate direction is expressed as

$$\Delta \epsilon^{sh}(t_n) = \epsilon_*^{sh} \cdot \frac{\Delta \phi(t_n)}{\phi_*} \quad (24)$$

ϵ_*^{sh} is the value of shrinkage strain at time infinity.

3. FINITE ELEMENT FORMULATION

A layered, compatible, sixteen degree of freedom rectangular plate bending element has been adopted, with the layering details as proposed by Wanchoo and May [8].

The prescribed displacement field for the element is expressed as

$$\{w\} = [A] \cdot \{a\} \quad (25)$$

where $[A]$ is a matrix of polynomial terms in x and y and $\{a\}$ is the vector of undetermined displacement coefficients. The generalised nodal deformations, consisting of displacements, slopes and twists, can be expressed as

$$\delta_i = \begin{bmatrix} w \\ \partial w / \partial x \\ \partial w / \partial y \\ \partial^2 w / \partial x \partial y \end{bmatrix} = \begin{bmatrix} A \\ \partial A / \partial x \\ \partial A / \partial y \\ \partial^2 A / \partial x \partial y \end{bmatrix} \cdot \{a\} = [G] \cdot \{a\} \quad (26)$$

The generalised element displacements are given by

$$\{q\} = [C^*] \cdot \{a\} \quad (27)$$

$[C^*]$ is the 16 x 16 'connectivity' matrix obtained by substituting the local coordinates of the four element nodes into the 4 x 16 $[G]$ matrix of Eq. 26.

The vector of curvatures can be written as

$$\{\kappa\} = [B] \cdot \{a\} \quad (28)$$

$$[B] = \begin{bmatrix} \partial^2 / \partial x^2 \\ \partial^2 / \partial y^2 \\ 2\partial^2 / \partial x \partial y \end{bmatrix} \cdot [A] \quad (29)$$

By substituting Eq. 27 into Eq. 28, the vector of curvatures can be expressed in terms of the generalised displacements:

$$\{\kappa\} = [B] \cdot [C^*]^{-1} \cdot \{q\} \quad (30)$$

For the typical layered element of Fig. 1, the vector of instantaneous strains in the biaxial stress state, $\{\epsilon^i\}$, at a depth z from the top surface of the slab is given by

$$\{\epsilon^i\} = \{\epsilon_0^i\} - z \cdot \{\kappa\} \quad (31)$$

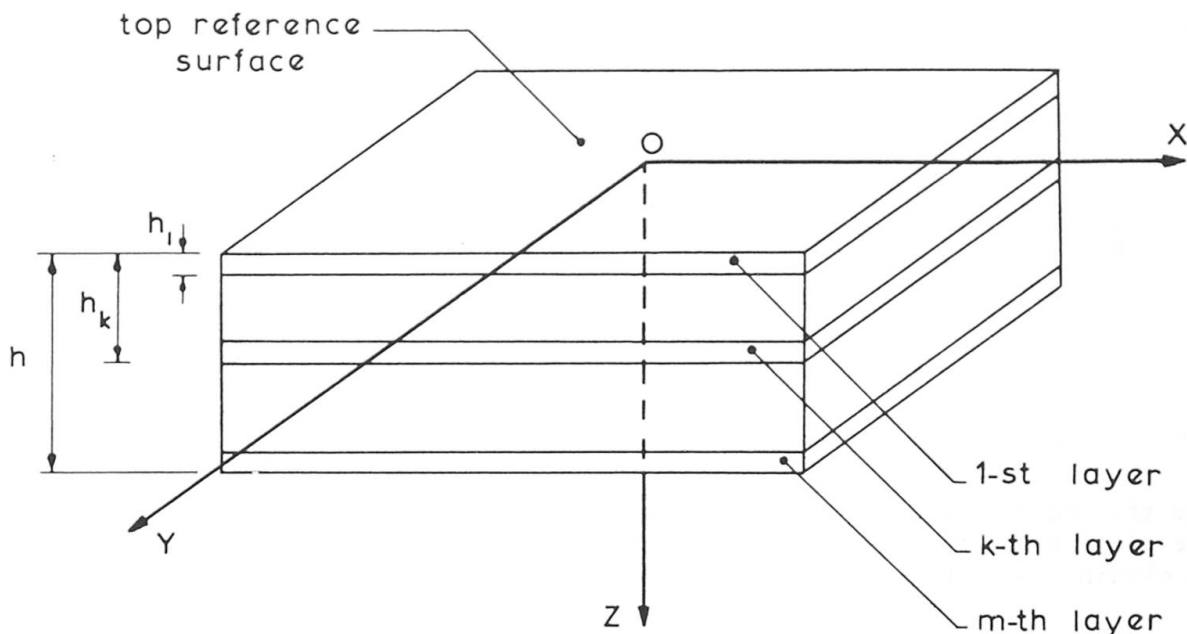


Fig. 1 Layered Finite Element Model

$\{\epsilon_0^i\}$ is the vector of instantaneous strains at the top reference surface.

By equating the sum of the in-plane forces of each layer to zero, the assumption of zero membrane forces is built into the basic element formulation:

$$\sum_{k=1}^m \Delta h_k ([C_k] \cdot \{\epsilon_0^i\} - z_k \cdot [C_k] \cdot \{\kappa\}) = 0 \quad (32)$$

In Eq. 32, $\Delta h_k = h_k - h_{k-1}$; $z_k = (h_k + h_{k-1})/2$; and $[C_k]$ represents the appropriate stress-instantaneous strain relation for the k-th layer and depends on the current material state and composition of the layer.

By rearranging and simplifying Eq. 33, $\{\epsilon_0^i\}$ is expressed as follows:

$$\{\epsilon_0^i\} = h \cdot [F] \cdot \{\kappa\} \quad (33)$$

$$[F] = \left[\sum_{k=1}^m \Delta h_k \cdot [C_k] \right]^{-1} \cdot \left[\sum_{k=1}^m \Delta h_k \cdot \frac{z_k}{h} \cdot [C_k] \right] \quad (34)$$

The $[F]$ matrix can readily be formulated from the current constitutive relations for each layer and their respective thicknesses and positions within the element.

The strain-displacement relationship for the k-th layer is obtained by substituting Eqs. 30 and 33 into Eq. 31:

$$\{\epsilon_k^i\} = [B_k^*] \cdot \{q\} \quad (35)$$

$$\begin{aligned} \text{where } [B_k^*] &= h \cdot \left[[F] \cdot [B] \cdot [C^*]^{-1} - \frac{z_k}{h} \cdot [B] \cdot [C^*]^{-1} \right] \\ &= [F^*] \cdot [B] \cdot [C^*]^{-1} \end{aligned} \quad (36)$$

It will be noted that these equations are quite general and are valid through all ranges of structural response within the limitations of small deflection plate theory. The various material behaviour states are conveniently accounted for by using the appropriate constitutive relation for $[C_k]$.



Equilibrium of the external loads $\{Q_k\}$ and the internal stresses is expressed by the volume integral

$$\{Q_k\} = \int_V [B_k^*]^T \cdot \{\sigma_k\} \cdot dV \quad (37)$$

$$\text{in which } \{\sigma_k\} = [C_k] \cdot \{\epsilon_k^i\} \quad (38)$$

and $\{\epsilon_k^i\}$ is the instantaneous component of total strain in the k-th layer.

By substituting Eqs. 35 and 38 into Eq. 37, we obtain the stiffness equation:

$$\{Q_k\} = \int_V [B_k^*] \cdot [C_k] \cdot [B_k^*] \cdot \{q\} \cdot dV = [K_k] \cdot \{q\} \quad (39)$$

The stiffness matrix of the k-th layer is $[K_k]$.

The stiffness of each layer is calculated and summed to obtain the stiffness of the element and the individual element stiffnesses are appropriately combined to obtain the global structural stiffness matrix.

When the stiffness of an element changes, due to a change in material state, the constitutive relation for the affected layer is appropriately modified. This results in a change of the stiffness of all layers within the element due to the reformulation of the $[F]$ matrix as defined by Eq. 34. The modified layer stiffnesses can be readily found and summed to obtain the updated element stiffness which adequately reflects the current material state.

The choice of the top surface of the slab as a reference surface (Fig. 1) is a convenient expedient in the element stiffness formulation and allows the use of elements of different thicknesses to be handled without complicating the analysis.

4. NON-LINEAR SOLUTION PROCEDURE

An incremental, piece-wise linear calculation procedure is used to model the non-linear and inelastic response which is characteristic of reinforced concrete behaviour under both instantaneous and sustained load.

4.1 Instantaneous Response

The most important contribution to the non-linear instantaneous behaviour of reinforced concrete slabs is the tensile cracking of the concrete. Cracking is treated analytically by increasing the external load in small increments and progressively changing the material properties of the layers as they become cracked. All other material non-linearities are treated in a similar manner.

The elastic structural stiffness matrix is first assembled and the linear elastic displacements produced by the full instantaneous load are determined. The state of stress in each layer is examined and the load is scaled down to the value which produces first cracking in the most highly stressed tensile layer. When cracking occurs, the concrete stress normal to the crack drops to zero, thus creating an unbalanced stress within the element. The stress-strain relation of the cracked layer is modified and the stress loss is transformed into an equivalent set of nodal forces, called transfer forces, $\{Q_{tr}\}$, using the principal of virtual work:

$$\{Q_{tr}\} = \int_V [B_k^*] \cdot \{\sigma_{tr}\} \cdot dV \quad (40)$$

where $\{\sigma_{tr}\}$ is the vector of transferred stresses in the global coordinate directions. The stiffness matrix is reformulated using the modified constitutive relation and equilibrium is restored within the model by applying the transfer forces to the structure using the 'initial stress' technique, as suggested by Zienkiewicz et al [12]. Additional displacements and associated stresses and strains are produced and the new state of stress in each layer is examined for further changes in material state. This iterative procedure continues until no further changes in material behaviour occur and convergence to the non-linear state of the slab at the current load level is obtained.

This process is repeated at each load level, as the load is increased in small increments from first cracking to the full instantaneous load. If the initial sustained load is less than the full instantaneous load, the slab is appropriately unloaded to the sustained load level and the time dependent solution procedure commences.

4.2 Time Dependent Response

Time dependent behaviour is calculated at a finite number of instants on the time scale, with the external load level only allowed to vary at these selected time instants.

During a typical time increment Δt , between the times t_n and t_{n+1} , the increments in creep strain due to the stresses existing at t_n and the shrinkage strain increments are calculated for each layer of each element. These 'creep' increments in strain are initially converted into 'relaxation' decrements in stress. The stress decrements are those which are needed at time t_{n+1} to restore the strains to their original values at time t_n . Horizontal equilibrium, temporarily lost due to the application of the relaxation stresses, is restored by transforming these stresses into nodal forces which, when applied, produce the additional displacements and stresses and strains which result from the time effects in the interval Δt . It will be noted that a relaxation type constitutive law could also be used directly in the first stage of this calculation.

The resulting state of stress in each layer at t_{n+1} is then examined for changes in local material behaviour. Checks are made to determine whether additional cracking has occurred, whether existing cracks have closed, whether the steel has yielded and so on. Any changes in material state within any layer are treated exactly as was described for instantaneous response. With equilibrium and strain compatibility ensured throughout, the time dependent behaviour of the slab at the end of the time increment, t_{n+1} , is obtained when the appropriate constitutive relation has been established for each element layer. Any changes in the external load level at the next time instant are analysed and the time dependent solution procedure for the next time increment commences.

The great advantage of this 'initial stress' relaxation approach is that the usual time consuming search techniques required to establish equilibrium and strain compatibility are eliminated. When the magnitudes of the creep and shrinkage strains in each layer have been determined and the material yield criteria are satisfied in all layers, the time dependent state of the slab is obtained directly. This solution procedure is general and does not rely on any one particular model of the creep and shrinkage characteristics of the concrete.



5. NUMERICAL RESULTS

5.1 Example 1

No well documented, laboratory controlled long-term tests of two-way reinforced concrete slabs have been found in the technical literature. However, field measurements on three in-service reinforced concrete slabs were presented by Taylor [7]. A flat slab floor in an open air carpark, constructed in 1965 and monitored for a period of 3½ years, has been selected for analysis.

Fig. 2 shows a plan of a typical internal panel of the slab, with the finite element mesh used in the analysis. The slab was 241 mm thick with 2440 x 2440 x 152 mm drop panels; the reinforcement layout and elastic material properties assumed in the analysis are as detailed by Taylor [7]. Transverse loading did not occur until 56 days after pouring; the total sustained load was taken to be the self weight of the slab, 5.75 kN/m². Full short-term live loading, 2.87 kN/m², was first applied approximately 70 days after first loading. This short-term load influences the long-term behaviour of the slab by causing additional cracking and hence an overall reduction of the slab stiffness. Due to the irreversible nature of cracking, the reduction of the slab stiffness remains even after the live load is removed.

Unfortunately, the creep and shrinkage characteristics of the concrete were not recorded but a relatively high shrinkage level was anticipated due to ineffective curing. Based on knowledge of the local concretes at that time, the following time dependent material properties were assumed:

$$\phi^* = 2.5; \alpha_d = 0.7; \alpha_n = 20; n = 4; \epsilon_*^{sh} = 0.0006 \text{ with 30\% of the total shrinkage assumed to have occurred in the 56 days prior to first loading.}$$

Theoretical and experimental time-deflection curves at the midpanel and the mid-point of the column centrelines are compared in Fig. 3. Despite the lack of accurate experimental data, the theoretical time-deflection curves are in good agreement with the actual slab response. A closer fit to the experimental curves could obviously be obtained by a suitable modification to the assumed shape of the constant stress creep curve and the final values of creep and shrinkage strains.

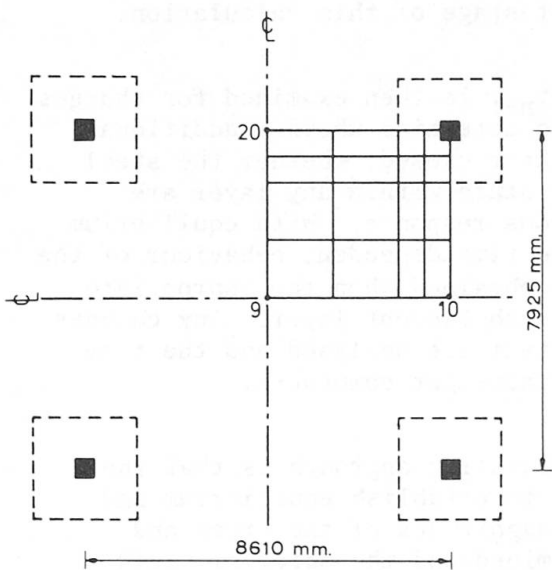


Fig. 2 Typical Internal Panel of Flat Slab Tested by Taylor [7].

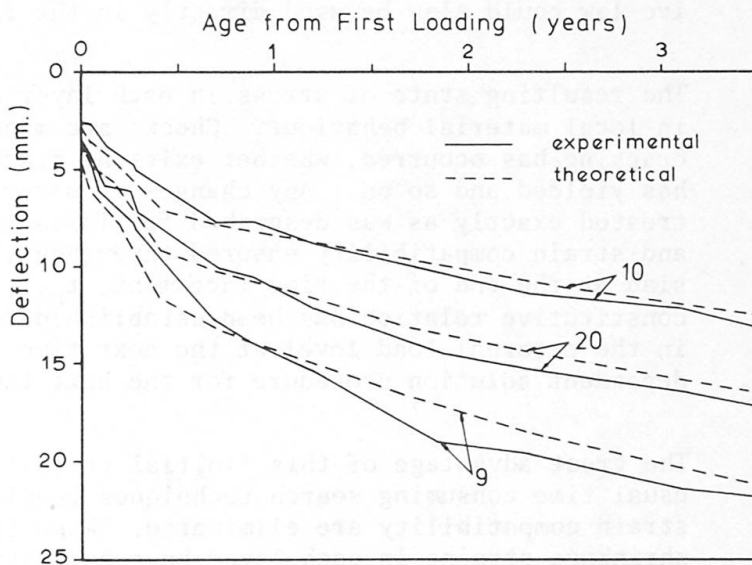


Fig. 3 Time-Deflection Curves for Flat Slab Tested by Taylor [7]

The ratio of long-term to short-term deflection at the midpanel was 5.0, which is considerably higher than the usual code multipliers. Under initial instantaneous load, the slab was essentially uncracked. However, considerable cracking occurred with time due to the gradual increase in tensile stresses caused by shrinkage. The loss of stiffness due to time dependent cracking, coupled with the direct effects of creep and shrinkage, results in the high long-term to short-term deflection ratio.

5.2 Example 2

To test further the accuracy of the proposed model, beams tested by Washa and Fluck [11] have been analysed. Three beams, all 127 mm deep and 305 mm wide with varying quantities of compression reinforcement, were tested over a period of 2½ years. Theoretical and experimental time-deflection curves at midspan are compared in Fig. 4. The theoretical curves were obtained using the creep and shrinkage data from companion loaded and unloaded test specimens. Again, agreement with test data is seen to be good.

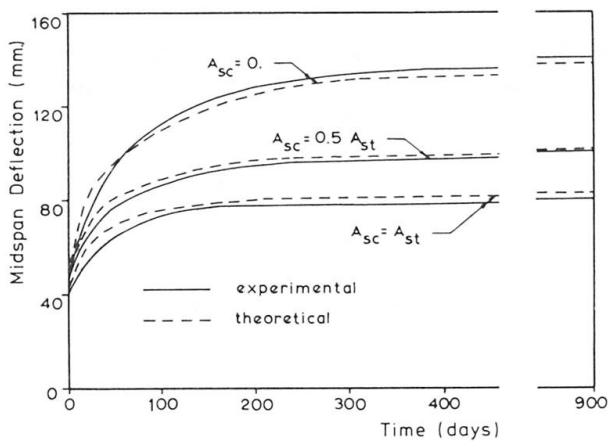


Fig. 4 Time-Deflection Curves for Beams Tested by Washa and Fluck, [11]

6. CONCLUSIONS

Computer simulation provides a rapid and inexpensive means for investigating the effects of creep and shrinkage on the time-dependent behaviour of reinforced concrete slabs. To provide spot checks on the accuracy of the computer model, supplementary experimental evidence is required. Unfortunately, well-documented experimental results of long-term slab behaviour are scarce and much work is required in this area.

Within the limits of available experimental results, the non-linear finite element model presented here accurately predicts both long-term and short-term behaviour of rectangular reinforced concrete slab systems under service loads. The idealised constitutive relations have represented well the various stages of material behaviour, while the element layering technique has made possible a close study of the state of stress as well as the orientation and height of cracks throughout the slab. The direct relaxation procedure is a particularly convenient method for determining strains and stresses at preselected time instants throughout the load history.

While good agreement with available test data has been obtained, it should be noted that the computer demands are relatively high. Economic considerations therefore limit the use of the model as an analytic tool for the practising engineer. However, as a research tool, the model provides an excellent opportunity to study the long-term behaviour of reinforced concrete slabs.



The slab simulation finite element program is at present being used in a parametric study of the relative importance of the various factors that influence long-term slab behaviour. The effects of creep, shrinkage, load level and reinforcement quantities on long-term slab deflections, the redistribution of internal actions, the extent and orientation of cracking and the ultimate strength of a variety of slab types are being considered. The results of this study will be presented in a second supplementary paper, with a view to the development of rational recommendations for the calculation of service load behaviour of reinforced concrete slabs.

7. REFERENCES

- [1] BRESLER, B., and SELNA, L.: "Analysis of Time-Dependent Behaviour of Reinforced Concrete Structures", Paper No. 5, Symposium on Creep of Concrete, ACI Publication SP-9, 1964.
- [2] FERRY BORGES, J., and ARANTES E. OLIVEIRA, E.R.: "Non-linear Analysis of Reinforced Concrete Structures", Publications, International Association for Bridge and Structural Engineering, Zürich, Vol. 23, 1963.
- [3] GILBERT, R.I., and WARNER, R.F.: "Non-linear Analysis of Reinforced Concrete Slabs with Tension Stiffening", UNICIV Report No. R-167, University of New South Wales, Kensington, Australia, January, 1977.
- [4] KUPFER, H., HILSDORF, H.K., and RÜSCH, H.: "Behaviour of Concrete under Biaxial Stresses", Journal ACI, Proc., Vol. 66, No. 8, 1969.
- [5] LAI, K.L., and WARNER, R.F.: "Non-linear Behaviour of Indeterminate Concrete Structures under Sustained Loading", UNICIV Report No. R-149, University of New South Wales, Kensington, Australia, November, 1975.
- [6] SCANLON, A.: "Time dependent Deflections of Reinforced Concrete Slabs", Ph.D. Thesis, University of Alberta, Edmonton, Alberta, Canada, 1971.
- [7] TAYLOR, P.J.: "The Initial and Long-Term Deflections of Reinforced Concrete Flat Slabs and Plates", M.E. Thesis, University of New South Wales, Kensington, Australia, 1971.
- [8] WANCHOO, M.K., and MAY, G.W.: "Cracking Analysis of Reinforced Concrete Plates", Journal of the Structural Division, ASCE, Vol. 101, No. ST1, 1975.
- [9] WARNER, R.F.: "Non-linear Creep in Concrete Columns", Final Report, Madrid Creep Symposium 1970, International Association for Bridge and Structural Engineering.
- [10] WARNER, R.F., and LAMBERT, J.H.: "Moment-Curvature-Time-Relations for Reinforced Concrete Beams", Publications, International Association for Bridge and Structural Engineering, Zürich, Vol. 34, 1974.
- [11] WASHA, G.W., and FLUCK, P.G.: "Effect of Compressive Reinforcement on the Plastic Flow of Reinforced Concrete Beams", Journal ACI, Proc., Vol. 49, 1952.
- [12] ZIENKIEWICZ, O.C., VALLIAPPAN, S., and KING, I.P.: "Elasto-Plastic Solutions of Engineering Problems, Initial Stress, Finite Element Approach", International Journal for Numerical Method in Engineering, Vol. 1, 1969.